

Addendum A: Plasmas and Tokamak Plasmas

Boris Andrews

Mathematical Institute, University of Oxford

March 15, 2023

Contents

1	An Overview	3
2	Modeling: Theory and Simulation	5
2.1	Particle Models	7
2.2	Kinetic Models	7
2.2.1	Non-Dimensionalization	10
2.3	Fluid Models	12

Nuclear fusion energy has the potential to provide a nearly unlimited source of clean and safe energy. Fusion reactions do not produce harmful greenhouse gases or long-lived radioactive waste and provide no risk of meltdown, making it a sustainable solution to meet the world’s growing demand for energy, from a stable and renewable source: hydrogen (and its isotopes). With the world’s energy demands continuously growing, fusion energy presents an attractive option for meeting these demands in a safe and sustainable manner.

Tokamaks—devices that use strong magnetic fields to contain and control plasmas at exceedingly high temperatures in order to achieve fusion—have proven over the past decades to be an effective leading option for producing and sustaining fusion. Unlike other similar devices, such as stellarators or Z-pinch devices, tokamaks have a relatively simple and well-studied design with comparatively straightforward engineering, making them easier to scale up to commercial-scale reactors. With its first plasma scheduled for late 2025 [1], the International Thermonuclear Experimental Reactor (ITER) will be the world’s largest tokamak [Mea09; 2], building towards DEMO: a proposed class of demonstration tokamak, with a target for commercial operation in the 2050s.

Because of these factors, tokamaks have received extensive funding and support from governments and private organizations around the world, making them potentially the most widely researched and developed fusion technology.

These factors combined make tokamaks one of the world’s best solutions for fusion energy, and arguably the most likely to achieve practical and commercial fusion reactor in the coming decades.

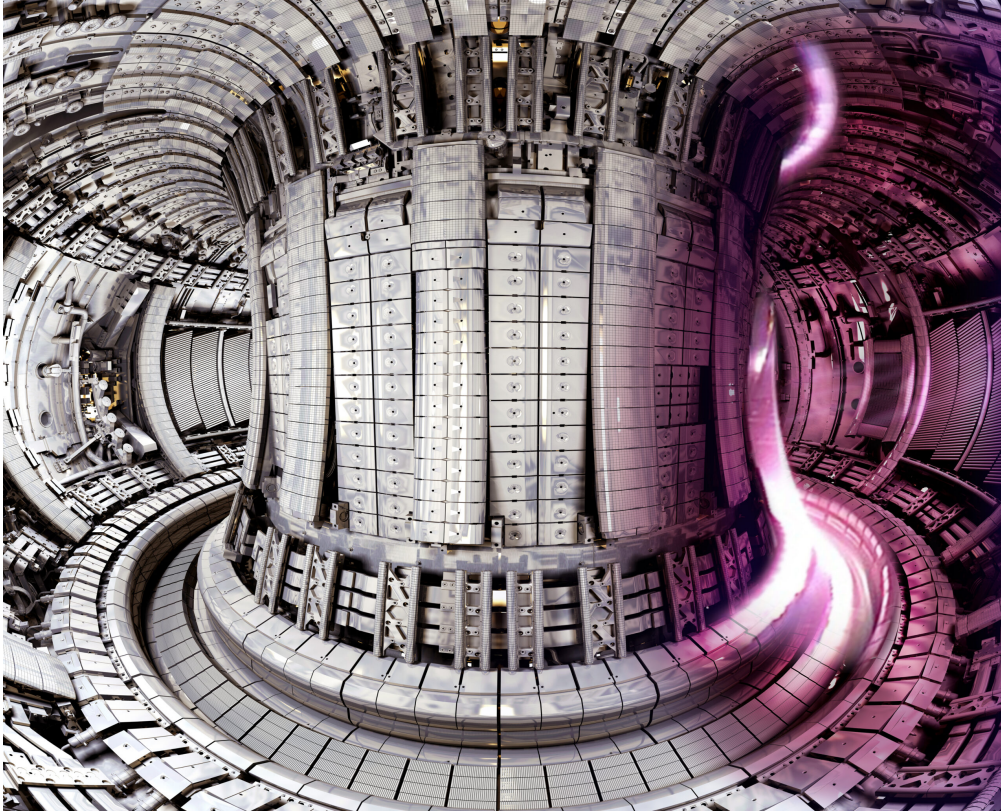


Figure 1: Illustration of the interior of the Joint European Torus (JET) reactor, located at the Culham Centre for Fusion Energy (CCFE). At the time of creation, JET was the largest tokamak in the world. (Source: CCFE)

The physical and numerical modeling of plasmas is a crucial area of study for tokamaks because it helps to understand and predict the behavior of the hot plasma in the containment vessel. The plasma must be maintained at high temperatures and densities in order to achieve fusion, and understanding its behavior is essential for optimizing the conditions in the tokamak and improving the fusion efficiency. Plasma modeling allows the simulation of various scenarios, such as changes in the magnetic fields or the heating methods used, and the observation of how these affects the plasma, allowing researchers and engineers to make informed decisions about how to increase the energy yield.

In addition, plasma modeling helps to identify and resolve potential problems that may arise during the fusion reaction, such as instabilities in the plasma or unwanted interactions with the chamber walls. By using computer simulations, these issues can be identified and resolved before they occur outside of the simulation, making the process safer and more efficient.

In this introduction, we present an overview of plasmas and their modeling, and the great difficulties these pose in tokamak-like environments.

BA: Would like references for the above paragraphs.

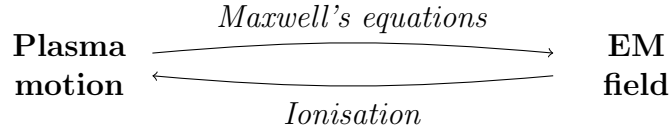
1 An Overview

What is a Plasma?

Definition 1.1 (Plasma). *“Plasma” refers here to an electrically charged fluid, typically occurring when a fluid is supplied with sufficient energy—from heating or an applied electromagnetic (EM) field—that a significant portion of the atoms **BA: (Not molecules?)** are ionized, causing the (positive) ion and (negative) electron phases to move independently.*

Plasma is one of the most abundant forms of matter in the universe [CL13], found most frequently in stars [Phi95; Asc06; Pie17] and similarly—as in our case—the star-like environments emulated in a tokamak.

While an applied EM field induces a current as it separates the two charged phases: the ions and electrons, the current similarly induces an EM field through Maxwell’s equations, creating a complex, coupled, nonlinear system.



What Distinguishes a Tokamak Plasma?

Certain properties characterize the plasma in a tokamak. The following figure are taken from [Wes00]:

- **Very high temperature:** Plasma temperatures within a tokamak are on the order of 10^8K , an order of magnitude *higher* than that in the center of the sun, at around $1.5 \times 10^7\text{K}$. **BA:** [Ref].
- **Very strong EM fields:** The EM fields used to ionize tokamak plasmas have strengths on the order 1T, with the world’s most powerful magnets being those employed in the world’s most powerful tokamaks. **BA:** [Ref]
- **Very low density:** Tokamak plasmas feature particle densities on the order of 10^{19}m^{-3} . The quantity of hydrogen gas used during a Joint European Torus (JET) pulse is often likened to the mass of a postage stamp. **BA:** [Ref]

Engineering constraints on the vessel walls often imply too that these plasmas both border onto complex boundaries with complex boundary condition, and can acquire high-levels of impurities from the chamber wall. While these can both have a large impact on the plasma dynamics, they will not be subject of this thesis.

Tokamak and Tokamak Plasma Structure

Consider now the structure of a tokamak, and with it the structure of the plasma contained within. Most crucially, the chamber is (approximately) rotationally symmetric in the vertical axis. Tokamak chambers are (almost always) *almost* toroidal in topology, albeit for the presence of divertors on the reactor wall: specialized regions where the plasma is directed away from the interior, allowing for the removal of impurities and heat.

As a result of Alfvén’s frozen-in flux theorem [Alf43], the plasma dynamics within the chamber are largely guided by the shape of the magnetic field (up to particle drifts) particularly in the ideal limit, as the plasma is “tied” to the magnetic field lines. One can therefore gain an understanding of the structure of the plasma within a tokamak by looking at the structure of the magnetic fields. (See Figure 2) The magnetic field within a tokamak has two components:

- **The toroidal field:** Generated by magnetic coils perpendicular to the length of the tokamak (parallel to the cross section in the diagram) and directed around the length of the tokamak (into the diagram).
- **The poloidal field:** Generated by magnetic coils around the length of the tokamak (into the diagram) and directed perpendicular to the toroidal field (parallel to the cross section in the diagram).

The combination of these two magnetic fields creates “flux surfaces”: 2D surfaces created by extending the magnetic field lines around the torus, within which the plasma is confined (labelled as “closed magnetic surfaces” and “open magnetic surfaces” in Figure 2). Many “local” models consider the plasma dynamics just along these flux surfaces.

The structure of these flux surfaces divide the tokamak plasma into several distinct regions, each with its own properties:

- **The core and edge regions:** The central regions of the plasma, where the flux surfaces are *closed* such that the plasma is fully contained. The core represents the center of this region, where the temperature and density are highest and the plasma is its most stable, and it is here where the majority of the fusion reactions occur.
- **The scrape-off layer (SOL) and divertor region:** Between the edge of the plasma and the tokamak walls, where the flux surfaces are *open* such that the plasma is diverted into a divertor. This is separated from the edge plasma by a flux surface called the “separatrix”, or “last closed flux surface” (LCFS). This is referred to as the divertor region when it enters a divertor, allowing for the removal of impurities and heat.
- **Private plasmas:** The small regions of the plasma contained around divertor, that do not form part of the SOL/divertor region.

The strength of the magnetic field and the shape of the flux surfaces can be controlled to optimize the confinement of the plasma and achieve the conditions necessary for fusion.

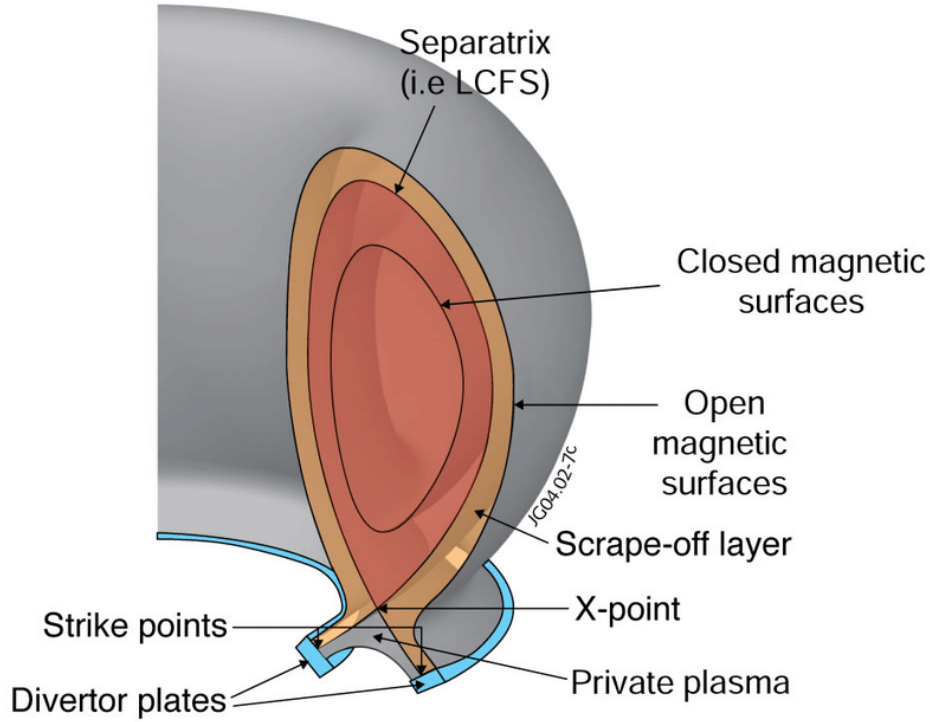


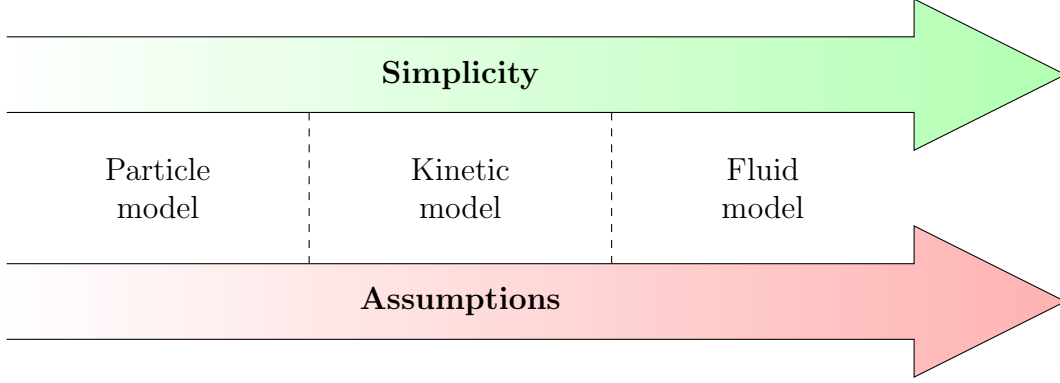
Figure 2: Cross-sectional diagram showing the magnetic field structure within a tokamak. (Source: European Fusion Development Agreement (EFDA))

2 Modeling: Theory and Simulation

When modeling fluids, there exist 3 classes of models (in so far as will be considered in this thesis):

1. Particle models (See Definition 2.1)
2. Kinetic models (See Definition 2.2)
3. Fluid models (See Definition 2.4)

When constructing a model, one starts from the full particle model, making assumptions on that model to reduce it to a kinetic model, and making further assumptions to reduce it to a fluid model. When progressing along this route, while the models become simpler in dimension, easing their analysis and numerical simulation, further and greater assumptions are required. One therefore finds a trade-off between the simplicity and approachability of the model, and its efficacy for the fluid being modeled.



For classical single phase, electrically-neutral fluids under typical real-world conditions, these assumptions are almost wholly valid, leading to the Navier–Stokes (NS) equations. When the same steps are applied for a quasineutral plasma, one derives the magnetohydrodynamic (MHD) equations.

Under typical tokamak-like conditions however, the steps required to go from the kinetic model to the fluid model do not hold nearly as well. Full fluid models like the MHD equations fail to capture highly influential “kinetic effects”, which are necessarily present only in the full kinetic model, which are highly influential in tokamak plasma dynamics. These include:

- Most plasma waves BA: [Ref]
- Most plasma/kinetic instabilities BA: [Ref]
- Landau damping/Bump-on-tail instabilities BA: [Ref]
- Leakage BA: [Ref]
- Kinetic structures (Beams/Double layers) BA: [Ref]
- Anisotropic pressures BA: [Ref]

Conversely, the full kinetic equation is 6-dimensional in position/velocity phase-space, and so its direct simulation is, in most situations, computationally intractable.

For practical purposes therefore, one requires some form of trade-off between a fully fluid and fully kinetic model. One common such technique is gyro-averaging, in the gyrokinetic model [How+06; PBP11; Abe+13] which has been seen to be effective in modeling many kinds of plasma turbulence [McK+01] but can exhibit non-physical behavior over long time periods BA: [Ref] among other physical weaknesses BA: [Ref]. Some gyroaveraging shall be considered when appropriate for psuedo-particle modeling in Chapter ?? BA: Other examples of such models? Ask Wayne.

In this thesis, we shall consider a coupled δf low-noise correction method. (See Chapter ??) To obtain this model, a derivation of the classical MHD model is presented in the following, with an analysis of the reasons for which it fails for highly kinetic tokamak plasmas.

2.1 Particle Models

Perhaps the most fundamental mathematical model for a plasma is the particle model.

Definition 2.1 (Particle model). *Here, “particle” models refer to those wherein every single particle is individually modeled.*

For a particle, indexed via the index $*_i$ in a phase indexed via the index $*_s$, denote the position $\mathbf{x}_{si}(t)$ and velocity $\mathbf{v}_{si}(t)$. Assuming the dominant forces acting on these particles are electromagnetic (EM) forces from either the background or other particles, $(\mathbf{x}_{si})_{si}$ and $(\mathbf{v}_{si})_{si}$ satisfy the systems of ODEs:

$$d\mathbf{x}_{si} = \mathbf{v}_{si} dt \quad (1)$$

$$m_s d\mathbf{v}_{si} = q_s [(\mathbf{E} - \mathbf{E}_{si}) + \mathbf{v}_{si} \wedge (\mathbf{B} - \mathbf{B}_{si})] dt \quad (2)$$

where \mathbf{E}_{si} , \mathbf{B}_{si} refer respectively to the contributions to the total electric, \mathbf{E} , and magnetic, \mathbf{B} , fields generated by the particle indexed $*_{si}$, and q_s , m_s respectively denote the particle charge and mass within the phase indexed $*_s$.

BA: Should maybe take note of background forces, i.e. gravity.

Naturally, this gives the most complete dynamical model for the plasma. On the tokamak scale however, with particle densities on the order of 10^{19}m^{-3} , modeling each particle individually is computationally intractable.

2.2 Kinetic Models

Definition 2.2 (Kinetic model). *Here, “kinetic” models refer to those wherein the distribution of particles positions and velocities is modelled through a single distribution function, as a function of both position and velocity.*

For each phase, s , define the distribution functions $(f_s(\mathbf{x}, \mathbf{v}; t))_s$ in the weak sense as

$$f_s(\mathbf{x}, \mathbf{v}; t) := \sum_i \delta^3[\mathbf{x} - \mathbf{x}_{si}(t)] \delta^3[\mathbf{v} - \mathbf{v}_{si}(t)], \quad (3)$$

where δ^3 denotes the 3-dimensional (3D) δ function. While working with such $(f_s)_s$ could *in theory* be used to model all the particles exactly and simultaneously, variations in \mathbf{x} of each f_s occur on the length scale of the distances between particles, i.e. on the order of 10^{-6}m in a tokamak plasma. We would therefore need a mesh resolution on a similar (if not finer) length scale to capture the physical nature of each f_s . Again: computationally infeasible.

For non-atomic scale simulations, such as those within a tokamak, the *precise* position of each particle is generally irrelevant to the general fluid behavior when not working on the atomic scale. The key idea of kinetic theory is to model this distribution function as a *random*

distribution, as one might do in Bayesian statistics to model a parameter that is known to be of fixed value as a random variable when full information on it remains unknown. Due to the scale of the number of particles for tokamak-scale simulations, the impact this assumption has on the efficacy of the model is negligible. One defines the 1-particle distribution functions, denoted here as $\left(\tilde{f}_s(\mathbf{x}, \mathbf{v}; t)\right)_s$, such that $\forall \phi(\mathbf{x}, \mathbf{v}; t)$,

$$\mathbb{E} \left\{ \int_{\mathbf{x}, \mathbf{v}; t} f_s(\mathbf{x}, \mathbf{v}; t) \phi(\mathbf{x}, \mathbf{v}; t) \right\} \left(= \sum_i \mathbb{E} \{ \phi(\mathbf{x}_{si}, \mathbf{v}_{si}; t) \} \right) = \int_{\mathbf{x}, \mathbf{v}; t} \tilde{f}_s(\mathbf{x}, \mathbf{v}; t) \phi(\mathbf{x}, \mathbf{v}; t) \quad (4)$$

Similarly the electromagnetic field must be modeled as a random distribution, with $\tilde{\mathbf{E}}(\mathbf{x}, t)$, $\tilde{\mathbf{B}}(\mathbf{x}, t)$ defined, such that $\forall \phi(\mathbf{x}, t)$,

$$\mathbb{E} \left\{ \int_{\mathbf{x}; t} \mathbf{E}(\mathbf{x}, t) \cdot \phi(\mathbf{x}, t) \right\} = \int_{\mathbf{x}; t} \tilde{\mathbf{E}}(\mathbf{x}, t) \cdot \phi(\mathbf{x}, t) \quad (5)$$

$$\mathbb{E} \left\{ \int_{\mathbf{x}; t} \mathbf{B}(\mathbf{x}, t) \cdot \phi(\mathbf{x}, t) \right\} = \int_{\mathbf{x}; t} \tilde{\mathbf{B}}(\mathbf{x}, t) \cdot \phi(\mathbf{x}, t) \quad (6)$$

We seek to cast the exact equations in $(f_s)_s$, \mathbf{E} , \mathbf{B} into ones in the distribution parameters $(\tilde{f}_s)_s$, $\tilde{\mathbf{E}}$, $\tilde{\mathbf{B}}$. To do so, once can apply the workflow as outline in Figure 3 to each equation.

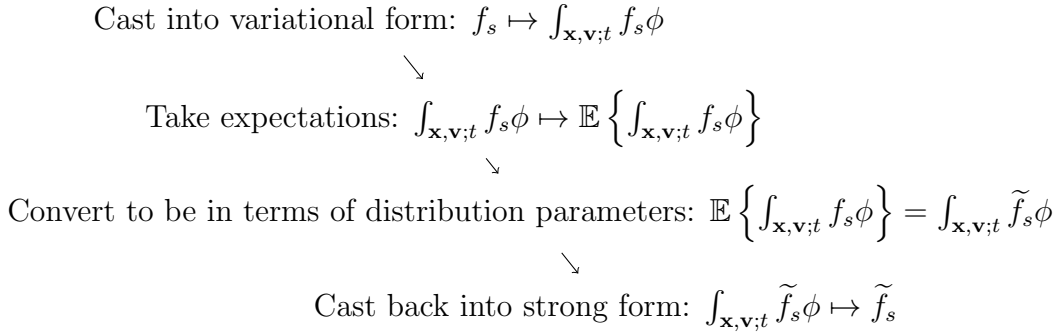


Figure 3: Diagram of workflow for construction of a kinetic model

Maxwell's Equations Since this process is entirely linear, Maxwell's equations—themselves linear—carry over identically:

$$\frac{1}{c^2} \partial_t \tilde{\mathbf{E}} = \nabla \wedge \tilde{\mathbf{B}} - \mu_0 \sum_s q_s \int_{\mathbf{v}} \tilde{f}_s \mathbf{v}, \quad \partial_t \tilde{\mathbf{B}} = -\nabla \wedge \tilde{\mathbf{E}}, \quad (7)$$

$$\frac{1}{c^2} \nabla \cdot \tilde{\mathbf{E}} = \mu_0 \sum_s q_s \int_{\mathbf{v}} \tilde{f}_s, \quad \nabla \cdot \tilde{\mathbf{B}} = 0. \quad (8)$$

where:

- c is the speed of light (in a vacuum), $c \approx 2.997 \dots \times 10^8 \text{ms}^{-1}$.

- μ_0 is the vacuum permeability, $\mu_0 \approx 1.257 \dots \times 10^{-6} \text{T}^2 \text{s}^2 \text{m}^1 \text{kg}^{-1}$.

BA: I should probably initially define Maxwell's equations in the previous particle models subsection, instead of first here.

Defining the charge and current densities, ρ_C and \mathbf{j} respectively, functions of \mathbf{x} and t :

$$\tilde{\rho}_C := \int_{\mathbf{v}} \tilde{f}_s q_s, \quad \tilde{\mathbf{j}} := \int_{\mathbf{v}} \tilde{f}_s q_s \mathbf{v}, \quad (9)$$

these can be written in the compact forms:

$$\frac{1}{c^2} \partial_t \tilde{\mathbf{E}} = \nabla \wedge \tilde{\mathbf{B}} - \mu_0 \tilde{\mathbf{j}}, \quad \partial_t \tilde{\mathbf{B}} = -\nabla \wedge \tilde{\mathbf{E}}, \quad (10)$$

$$\frac{1}{c^2} \nabla \cdot \tilde{\mathbf{E}} = \mu_0 \tilde{\rho}_C, \quad \nabla \cdot \tilde{\mathbf{B}} = 0. \quad (11)$$

Boltzmann Equations The evolution equations for $(f_s)_s$ or $(\tilde{f}_s)_s$ are not as simple, due to their non-linearity. When applying this technique one derives the “*Boltzmann equations*”, BA: [Ref]

$$\partial_t \tilde{f}_s + \nabla_{\mathbf{x}} \cdot [\tilde{f}_s \mathbf{v}] + \frac{q_s}{m_s} \nabla_{\mathbf{v}} \cdot [\tilde{f}_s (\tilde{\mathbf{E}} + \mathbf{v} \wedge \tilde{\mathbf{B}})] = \frac{q_s}{m_s} \sum_{s'} q_{s'} \nabla_{\mathbf{v}} \cdot \mathbf{C}_{ss'}, \quad (12)$$

where the collision terms $(\mathbf{C}_{ss'})_{ss'}$ are terms characterising the Coulomb collisions, defined as

$$\mathbf{C}_{ss'} [\tilde{f}_s, \tilde{f}_{s'}, \tilde{f}_s \tilde{f}_{s'}] (\mathbf{x}, \mathbf{v}; t) := \int_{\mathbf{x}' \neq \mathbf{x}, \mathbf{v}'; t'} \left(\tilde{f}_s(\mathbf{x}, \mathbf{v}; t) \tilde{f}_{s'}(\mathbf{x}', \mathbf{v}'; t') - \tilde{f}_s \tilde{f}_{s'}[(\mathbf{x}, \mathbf{v}; t), (\mathbf{x}', \mathbf{v}'; t')] \right) [\mathbf{k}_{\mathbf{E}}(\mathbf{x}' - \mathbf{x}, \mathbf{v}'; t' - t) + \mathbf{v} \wedge \mathbf{k}_{\mathbf{B}}(\mathbf{x}' - \mathbf{x}, \mathbf{v}'; t' - t)], \quad (13)$$

where in turn:

- $\mathbf{k}_{\mathbf{E}}, \mathbf{k}_{\mathbf{B}}$, as functions in $\mathbf{x}', \mathbf{v}', t'$, are kernels of the electric and magnetic field, defined as the electric and magnetic fields produced at the origin by a unit point charge at position \mathbf{x}' with velocity \mathbf{v}' at time $t' \in [-\frac{1}{c}\|\mathbf{x}'\|, 0]$. BA: (Explicit definition for $\mathbf{k}_{\mathbf{E}}, \mathbf{k}_{\mathbf{B}}$? Not really needed for the theory.)
- The 2-particle distributions functions $\left(\widetilde{f_{s_1} f_{s_2}}[(\mathbf{x}_1, \mathbf{v}_1; t_1), (\mathbf{x}_2, \mathbf{v}_2; t_2)] \right)_{s_1 s_2}$ are defined such that $\forall \phi[(\mathbf{x}_1, \mathbf{v}_1; t_1), (\mathbf{x}_2, \mathbf{v}_2; t_2)]$,

$$\begin{aligned} \mathbb{E} \left\{ \int_{\mathbf{x}_1, \mathbf{v}_1; t_1} \int_{\mathbf{x}_2, \mathbf{v}_2; t_2} f_{s_1}(\mathbf{x}_1, \mathbf{v}_1; t_1) f_{s_2}(\mathbf{x}_2, \mathbf{v}_2; t_2) \phi[(\mathbf{x}_1, \mathbf{v}_1; t_1), (\mathbf{x}_2, \mathbf{v}_2; t_2)] \right\} \\ = \sum_{i_1, i_2} \mathbb{E} \{ \phi[(\mathbf{x}_{s_1 i_1}, \mathbf{v}_{s_1 i_1}; t_1), (\mathbf{x}_{s_2 i_2}, \mathbf{v}_{s_2 i_2}; t_2)] \} \\ = \int_{\mathbf{x}_1, \mathbf{v}_1} \int_{\mathbf{x}_2, \mathbf{v}_2} \widetilde{f_{s_1} f_{s_2}}[(\mathbf{x}_1, \mathbf{v}_1; t_1), (\mathbf{x}_2, \mathbf{v}_2; t_2)] \phi[(\mathbf{x}_1, \mathbf{v}_1; t_1), (\mathbf{x}_2, \mathbf{v}_2; t_2)]. \quad (14) \end{aligned}$$

These capture some of the nature of how the positions of pairs of particles are correlated.

For a full derivation of (12) see Appendix ??.

Obviously this system is not closed, as it in turn is dependent on $\left(\widetilde{f_{s_1} f_{s_2}}\right)_{s_1 s_2}$; this is referred to as the “*closure problem*”. Different approximations to $\left(\widetilde{f_{s_1} f_{s_2}}\right)_{s_1 s_2}$ lead to different collisional forces and collision operators in the Boltzmann equation.

From here, we shall drop the tildes $\widetilde{*}$ on $\widetilde{f_s}$, $\widetilde{\mathbf{E}}$, $\widetilde{\mathbf{B}}$, $\widetilde{\rho_C}$, $\widetilde{\mathbf{j}}$, as we shall not be returning to the particle model. Together this system can be referred to as the Boltzmann–Maxwell system.

2.2.1 Non-Dimensionalization

Consider now a non-dimensionalization of Maxwell’s equation (10–11) and the Boltzmann equations (12).

By the problem specification, the physical constants:

$$(q_s)_s, \quad (m_s)_s, \quad (15)$$

are given by the parameters in the constituent phases. Further denoting an estimate for the general scale of a variable, $*$, with an overbar, $\overline{*}$, the following quantities are given too by the problem specification within the tokamak:

$$\overline{t}, \quad \overline{\mathbf{x}}, \quad (\overline{n_s})_s, \quad \overline{\mathbf{B}}, \quad (16)$$

where n_s denote the particle density of phase s , $n_s := \int_{\mathbf{v}} f_s$. From this definition,

$$\overline{f_s} := \frac{\overline{n_s}}{\overline{\mathbf{v}}^3}. \quad (17)$$

$\overline{\mathbf{v}}$ will scale to achieve dominant balance in the Boltzmann equations (12), however this shall be discussed in Subsection 2.3. For now, it shall be assumed known.

Define also:

- The cyclotron frequency in phase s ,

$$\Omega_s := \frac{q_s}{m_s} \cdot \overline{\mathbf{B}}. \quad (18)$$

- The (effective) mean free for particles in phase s , between particles in phase s'

$$\lambda_{ss'} := \frac{m_s}{q_s q_{s'}} \cdot \frac{\overline{n_s}}{\overline{\mathbf{v}} \overline{C_{ss'}}}. \quad (19)$$

These invoke the dimensionless quantities in Figure 4.

Name	Symbol	Value	Ratio
(Light) Mach number	M	$\bar{\mathbf{v}}/c$	(Particle : Light) speed
Strouhal number	St	$\bar{\mathbf{x}}/\bar{t}\bar{\mathbf{v}}$	(Reference : Kinetic) frequency
Cyclotron number(s)	Cy _s	$\Omega_s \bar{t}$	(Cyclotron : Reference) frequency
Knudsen number(s)	Kn _{ss'}	$\bar{\mathbf{x}}/\lambda_{ss'}$	(Reference : Mean free path) length

Figure 4: Dimensionless quantities in the Boltzmann–Maxwell system.

Maxwell’s equation (10–11) We suppose $\bar{\mathbf{B}}$ is given by the problem specification while $\bar{\mathbf{E}}$ is *not*, as the driving electromagnetic field within a tokamak is typically a magnetic field only, with the electric field induced internally through Maxwell’s equations. As the magnetic field, \mathbf{B} , varies during a simulation, the electric field must change to balance this varying magnetic field in Faraday’s law, $\partial_t \mathbf{B} = -\nabla \wedge \mathbf{E}$, such that the electric field scale, $\bar{\mathbf{E}}$, is given as

$$\bar{\mathbf{E}} = \text{St} \bar{\mathbf{v}} \bar{\mathbf{B}}. \quad (20)$$

As such, up to variation in St, the electric and magnetic Lorentz forces are comparable in magnitude.

Similarly, according to Ampère’s law, $\frac{1}{c^2} \partial_t \mathbf{E} = \nabla \wedge \mathbf{B} - \mu_0 \mathbf{j}$, the curl in the applied magnetic field, $\nabla \wedge \mathbf{B}$, must be balanced by the induced current density, \mathbf{j} . Thus the current density scale, $\bar{\mathbf{j}}$, is given as

$$\bar{\mathbf{j}} = \frac{1}{\mu_0} \cdot \frac{\bar{\mathbf{B}}}{\bar{\mathbf{x}}}. \quad (21)$$

Finally, according to Gauss’s law, $\frac{1}{c^2} \nabla \cdot \mathbf{E} = \mu_0 \rho_C$, the divergence in the induced electric field, $\nabla \cdot \mathbf{E}$, must be balanced by the induced charge density, ρ_C . Thus the current density scale, $\bar{\rho}_C$, is given as

$$\bar{\rho}_C = \text{St} M^2 \cdot \frac{1}{\mu_0} \cdot \frac{\bar{\mathbf{B}}}{\bar{\mathbf{x}} \bar{\mathbf{v}}}. \quad (22)$$

One can thus non-dimensionalize Maxwell’s equations as:

$$M^2 \partial_t \mathbf{E} = \nabla \wedge \mathbf{B} - \mathbf{j}, \quad \partial_t \mathbf{B} = -\nabla \wedge \mathbf{E}, \quad (23)$$

$$\nabla \cdot \mathbf{E} = \rho_C, \quad \nabla \cdot \mathbf{B} = 0. \quad (24)$$

Boltzmann equations (12) One can non-dimensionalize the Boltzmann equations (about the convective $\nabla_{\mathbf{x}} \cdot [f_s \mathbf{v}]$ terms) as

$$\text{St} \partial_t f_s + \nabla_{\mathbf{x}} \cdot [f_s \mathbf{v}] + \text{St} \text{Cy}_s \nabla_{\mathbf{v}} \cdot [f_s (\text{St} \mathbf{E} + \mathbf{v} \wedge \mathbf{B})] = \sum_{s'} \text{Kn}_{ss'} \nabla_{\mathbf{v}} \cdot \mathbf{C}_{ss'}. \quad (25)$$

From here, the non-dimensionalized system shall be assumed.

Name	Symbol	Value	Ratio
Fluid Reynolds number	Re_f	[See below]	(Inertial : Viscous) forces
Plasma beta	β	$2\mu_0 \cdot \max_s \{m_s \bar{n}_s\} \cdot \bar{\mathbf{v}}^2 / \bar{\mathbf{B}}^2$	(Plasma : Magnetic) pressure

Figure 5: Dimensionless quantities in the MHD system.

Lemma 2.3 (Momentum and energy conservation on $(\mathbf{C}_{ss'})_{ss'}$). *The following two identities hold on $(\mathbf{C}_{ss'})_{ss'}$:*

$$\int_{\mathbf{x}} \left[\sum_{s,s'} \text{Kn}_{ss'} \frac{m_s \bar{n}_s}{\max_s \{m_s \bar{n}_s\}} \int_{\mathbf{v}} \mathbf{C}_{ss'} \right] = \mathbf{0}, \quad \int_{\mathbf{x}} \left[\sum_{s,s'} \text{Kn}_{ss'} \frac{m_s \bar{n}_s}{\max_s \{m_s \bar{n}_s\}} \int_{\mathbf{v}} \mathbf{C}_{ss'} \cdot \mathbf{v} \right] = 0. \quad (26)$$

Proof. These results are immediate from conservation of momentum and energy over the whole domain. \square

2.3 Fluid Models

Definition 2.4 (Fluid model). *Here, “fluid” models refer to those wherein the system is reduced from one in both position and velocity space (and time) to one in just position space (and time) through some kind of approximation to the distribution function.*

Recall the non-dimensionalized Boltzmann equations (25):

$$\text{St} \partial_t f_s + \nabla_{\mathbf{x}} \cdot [f_s \mathbf{v}] + \text{St} \text{Cy}_s \nabla_{\mathbf{v}} \cdot [f_s (\text{St} \mathbf{E} + \mathbf{v} \wedge \mathbf{B})] = \sum_{s'} \text{Kn}_{ss'} \nabla_{\mathbf{v}} \cdot \mathbf{C}_{ss'}$$

Using some approximations to the 2-particle distribution functions, $(f_{ss'})_{ss'}$, as functions of the 1-particle distribution functions, $(f_s, f_{s'})_{ss'}$, suppose from here that the collision operators, $(\mathbf{C}_{ss'})_{ss'}$, are written as functions of the 1-particle distribution functions only, as

$$\mathbf{C}_{ss'}[f_s, f_{s'}](\mathbf{x}, \mathbf{v}; t). \quad (27)$$

This quantifies the collision operator model, bringing a solution to the closure problem. Most often, these 2-particle distribution function approximations are defined implicitly through the collision operator approximation.

To transfer from the fully kinetic model—the Boltzmann equations (25)—to a fluid model, one must make certain assumption. Various dimension quantities will be invoked, as defined in Figure 5.

Assumption 1: Leading-Order Locality of the Collision Operators

Fluid models consider scales wherein the dominant collisional effects are local in space and time. It is assumed that $(\mathbf{C}_{ss'})_{ss'}$ are dominated by the local contributions of $(f_s, f_{s'})$ at each \mathbf{x} and t ; that is to say that, up to leading order,

$$\mathbf{C}_{ss'}[f_s, f_{s'}](\mathbf{x}, \mathbf{v}; t) \sim \mathbf{C}_{ss'}^{(0)}[f_s|_{\mathbf{x};t}, f_{s'}|_{\mathbf{x};t}](\mathbf{x}, \mathbf{v}; t) \quad (28)$$

for some $(\mathbf{C}_{ss'}^{(0)})_{ss'}$. Defining the dimensionless quantities

$$\text{Re}_{f_{ss'}} = \frac{1}{\text{Kn}_{ss'} \left(\mathbf{C}_{ss'} - \mathbf{C}_{ss'}^{(0)} \right)}, \quad (29)$$

one equivalently requires that $\text{Kn}_{ss'} \text{Re}_{f_{ss'}} \gg 1, \forall s, s'$. This motivates the definition of Re_f in Figure 5.

Defining

$$\delta \mathbf{C}_{ss'} := \text{Kn}_{ss'} \text{Re}_{f_{ss'}} \left(\mathbf{C}_{ss'} - \mathbf{C}_{ss'}^{(0)} \right), \quad (30)$$

$(\delta \mathbf{C}_{ss'})_{ss'}$ are dimensionless terms that each capture the non-local, viscous collisional effects.

This extends the results of Lemma 2.3:

Lemma 2.5 (Momentum and energy conservation on $(\mathbf{C}_{ss'}^{(0)})_{ss'}$). *The following two identities hold on $(\mathbf{C}_{ss'}^{(0)})_{ss'}$:*

$$\sum_{s,s'} \text{Kn}_{ss'} \frac{m_s \bar{n}_s}{\max_s \{m_s \bar{n}_s\}} \int_{\mathbf{v}} \mathbf{C}_{ss'}^{(0)} = \mathcal{O}[\epsilon], \quad \sum_{s,s'} \text{Kn}_{ss'} \frac{m_s \bar{n}_s}{\max_s \{m_s \bar{n}_s\}} \int_{\mathbf{v}} \mathbf{C}_{ss'}^{(0)} \cdot \mathbf{v} = \mathcal{O}[\epsilon], \quad (31)$$

where

$$\epsilon := \max_{s,s'} \left\{ \frac{m_s \bar{n}_s}{\text{Re}_{f_{ss'}}} \right\} / \max_s \{m_s \bar{n}_s\} \quad (32)$$

Proof. By Lemma 2.3:

$$\begin{aligned} \int_{\mathbf{x}} \left[\sum_{s,s'} \text{Kn}_{ss'} \frac{m_s \bar{n}_s}{\max_s \{m_s \bar{n}_s\}} \int_{\mathbf{v}} \mathbf{C}_{ss'}^{(0)} \right] &= \mathcal{O}[\epsilon], \\ \int_{\mathbf{x}} \left[\sum_{s,s'} \text{Kn}_{ss'} \frac{m_s \bar{n}_s}{\max_s \{m_s \bar{n}_s\}} \int_{\mathbf{v}} \mathbf{C}_{ss'}^{(0)} \cdot \mathbf{v} \right] &= \mathcal{O}[\epsilon]. \end{aligned} \quad (33)$$

Since $(\mathbf{C}_{ss'}^{(0)})_{ss'}$ are local in space, the only way for this integral identity necessarily to hold is if it holds pointwise in space, for each \mathbf{x} . \square

Accordingly, define Re_f : (See Figure 5)

$$\text{Re}_f := \frac{1}{\epsilon} = \max_s \{m_s \bar{n}_s\} / \max_{s,s'} \left\{ \frac{m_s \bar{n}_s}{\text{Re}_{f_{ss'}}} \right\} \quad (34)$$

It will be assumed for simplicity from here that $\text{Re}_f > 1$, as is typical for highly turbulent tokamak plasmas.

Corollary 2.6 (Phase-restricted momentum and energy conservation on $(\mathbf{C}_{ss'}^{(0)})_{ss'}$). *As corollaries to Lemma 2.5:*

- $\forall s$, the following two identities hold on $\mathbf{C}_{ss}^{(0)}$:

$$\int_{\mathbf{v}} \text{Kn}_{ss} \mathbf{C}_{ss}^{(0)} = \mathcal{O}[\epsilon_s], \quad \int_{\mathbf{v}} \text{Kn}_{ss} \mathbf{C}_{ss}^{(0)} \cdot \mathbf{v} = \mathcal{O}[\epsilon_s], \quad (35)$$

where

$$\epsilon_s := \frac{1}{\text{Re}_{f_{ss}}} \quad (36)$$

- $\forall s, s'$, the following two identities hold on $\mathbf{C}_{ss'}^{(0)}$ and $\mathbf{C}_{s's}^{(0)}$:

$$\begin{aligned} \int_{\mathbf{v}} \left[\text{Kn}_{ss'} \frac{m_s \bar{n}_s}{\max_{s_1 \in \{s, s'\}} \{m_{s_1} \bar{n}_{s_1}\}} \mathbf{C}_{ss'}^{(0)} + \text{Kn}_{s's} \frac{m_{s'} \bar{n}_{s'}}{\max_{s_1 \in \{s, s'\}} \{m_{s_1} \bar{n}_{s_1}\}} \mathbf{C}_{s's}^{(0)} \right] &= \mathcal{O}[\epsilon_{ss'}], \\ \int_{\mathbf{v}} \left[\text{Kn}_{ss'} \frac{m_s \bar{n}_s}{\max_{s_1 \in \{s, s'\}} \{m_{s_1} \bar{n}_{s_1}\}} \mathbf{C}_{ss'}^{(0)} + \text{Kn}_{s's} \frac{m_{s'} \bar{n}_{s'}}{\max_{s_1 \in \{s, s'\}} \{m_{s_1} \bar{n}_{s_1}\}} \mathbf{C}_{s's}^{(0)} \right] \cdot \mathbf{v} &= \mathcal{O}[\epsilon_{ss'}], \end{aligned} \quad (37)$$

where

$$\epsilon_{ss'} := \max_{s_1, s_2 \in \{s, s'\}} \left\{ \frac{m_{s_1} \bar{n}_{s_1}}{\text{Re}_{f_{s_1 s_2}}} \right\} / \max_{s_1 \in \{s, s'\}} \{m_{s_1} \bar{n}_{s_1}\} \quad (38)$$

Proof. When observing just a subset of the phases, Lemma 2.5 must still hold true:

- The first results hold true by restriction to the phase s .
- The second results hold true as a corollary of the first, by restriction to the phases s and s' .

□

Assumption 2: EM vs. Collisions Dominant Balance

Consider now the scale of the dimensionless quantities in (25), to consider which terms are in dominant balance.

Consider a typical JET reactor pulse, with a predominant (positive) deuterium ion (indexed via $s \mapsto +$) and (negative) electron (indexed via $s \mapsto -$) phase:

$$q_{\pm} \approx \pm 1.602 \dots \times 10^{-19} \text{kg s}^{-1} \text{T}^{-1}, \quad (39)$$

$$m_+ \approx 3.344 \dots \times 10^{-27} \text{kg}, \quad m_- \approx 9.109 \dots \times 10^{-31} \text{kg}. \quad (40)$$

The following parameters for the JET reactor are listed in Chapters 2 and 4 of [Wes00]:¹

$$\bar{\mathbf{x}} \approx 2.5 \text{m}, \quad \bar{n}_{\pm} \approx 10^{19} \text{m}^{-3}, \quad \bar{\mathbf{B}} \approx 3.5 \text{T}. \quad (41)$$

For the remaining two scales:

¹ $\bar{\mathbf{x}}$ is evaluated as twice the minor radius, 1.25m.

- \bar{t} shall be taken as equal to $\bar{\mathbf{x}}/\bar{\mathbf{v}}$, such that $\text{St} = 1$, i.e. the model is on the convective timescale.
- $\bar{\mathbf{v}}$ shall be taken, as stated above, to achieve dominant balance.

While the Knudsen numbers, $\text{Kn}_{\pm\pm}$, scale *with* $\bar{\mathbf{v}}$, the cyclotron numbers Cy_{\pm} scale *inversely*. At a certain velocity scale, $\bar{\mathbf{v}}$, therefore, a balance will be achieved, where $\max\{|\text{Cy}_{\pm}|\} = \max\{\text{Kn}_{\pm\pm}\}$. When such a balance is achieved, as will be seen after their evaluation below, $\max\{|\text{Cy}_{\pm}|\} = \max\{\text{Kn}_{\pm\pm}\} \gg 1$, implying this balance is dominant. This equilibrium velocity scale can be evaluated as the thermal velocity scale at operational temperature,

$$\bar{\mathbf{v}} \approx \sqrt{\frac{k_B}{m_+} \cdot \bar{\theta}}, \quad (42)$$

where k_B is the Boltzmann constant, $k_B \approx 1.381 \dots \times 10^{-23} \text{m}^2 \text{kgK}^{-1} \text{s}^{-2}$, and θ denotes the temperature. For $\bar{\theta} \approx 1.5 \dots \times 10^8$ as given by [Wes00], $\bar{\mathbf{v}} \approx 7.869 \dots \times 10^5 \text{ms}^{-1}$.

BA: (786924.39206)

The dimensionless quantities in Figure 4 thus evaluate as:

$$M \approx 2.625 \dots \times 10^{-3} \quad (43)$$

$$\text{St} = 1 \quad (44)$$

$$|\text{Cy}_+| \approx \max\{\text{Kn}_{++}, \text{Kn}_{+-}\} \approx 5.327 \dots \times 10^2 \quad (45)$$

$$|\text{Cy}_-| \approx \max\{\text{Kn}_{--}, \text{Kn}_{-+}\} \approx 1.957 \dots \times 10^6 \quad (46)$$

...

Under typical tokamak conditions therefore, one can expect the Boltzmann equations for either phase are dominated by the EM terms, $\text{Cy}_{\pm} \nabla_{\mathbf{v}} \cdot [f_{\pm} (\mathbf{E} + \mathbf{v} \wedge \mathbf{B})]$, and the collisional terms, $\text{Kn}_{\pm 1 \pm 2} \nabla_{\mathbf{v}} \cdot \mathbf{C}_{\pm 1 \pm 2}$, by a factor of Cy_{\pm} . The Boltzmann equations then take the leading-order forms:

$$\text{Cy}_{\pm} \nabla_{\mathbf{v}} \cdot [f_{\pm} (\mathbf{E} + \mathbf{v} \wedge \mathbf{B})] = \text{Kn}_{\pm\pm} \nabla_{\mathbf{v}} \cdot \mathbf{C}_{\pm\pm} + \text{Kn}_{\pm\mp} \nabla_{\mathbf{v}} \cdot \mathbf{C}_{\pm\mp} + \mathcal{O}[1] \quad (47)$$

$$\nabla_{\mathbf{v}} \cdot [\text{Cy}_{\pm} f_{\pm} (\mathbf{E} + \mathbf{v} \wedge \mathbf{B}) - \text{Kn}_{\pm\pm} \mathbf{C}_{\pm\pm} - \text{Kn}_{\pm\mp} \mathbf{C}_{\pm\mp}] = \mathcal{O}[1] \quad (48)$$

This approximation holds true only to an accuracy of $1/\text{Cy}_{\pm}$. While it is true that in each phase, $\text{Cy}_{\pm} > 1$, these values are *very small* in comparison to those that would typically be found in other comparable kinetic systems. This is particularly true in the ion phase, with Cy_+ at less than 10^3 in magnitude; compare with the equivalent factor of around 10^{11} for the hydrogen phase in the full solar corona.

It is primarily this factor that is responsible for the shortcoming of the fluid approximation for tokamak plasmas, and the high influence of kinetic effects on their dynamics.

Remark (Justification for the non-relativistic model). *Up until now, a non-relativistic model has been assumed. Observing that $M \ll 1$, i.e.. $\bar{\mathbf{v}} \ll c$, we see that this is in general a fair assumption. Relativistic effects are known to have some effects on tokamak plasma dynamics however, due to their impact on the very-high energy/speed tails of the distribution functions.*

BA: [Ref]

The Resultant Spatially-Local System

One seeks now to leverage these 2 assumptions to derive a fluid model in the following (non-dimensionalized) functions of \mathbf{x} and t only:

$$\text{Mass density, } \rho_M(\mathbf{x}; t) := \int_{\mathbf{v}} \left[f_+ + f_- \frac{m_-}{m_+} \right] \quad (49)$$

$$\text{Charge density, } \rho_C(\mathbf{x}; t) := \frac{\beta C y_+}{2M^2} \int_{\mathbf{v}} [f_+ - f_-] \quad (50)$$

$$\text{Total momentum, } \mathbf{p}(\mathbf{x}; t) := \int_{\mathbf{v}} \left[f_+ + f_- \frac{m_-}{m_+} \right] \mathbf{v} \quad (51)$$

$$\text{Total energy, } E(\mathbf{x}; t) := \int_{\mathbf{v}} \left[f_+ + f_- \frac{m_-}{m_+} \right] \frac{1}{2} \|\mathbf{v}\|^2 \quad (52)$$

with β defined: (See Figure 5)

$$\beta := 2\mu_0 m_+ \cdot \frac{\bar{n}_+ \bar{\mathbf{v}}^2}{\bar{\mathbf{B}}^2} \quad (53)$$

With $m_- \ll m_+$, one can write:

$$\rho_M(\mathbf{x}; t) = \int_{\mathbf{v}} f_+ + \mathcal{O} \left[\frac{m_-}{m_+} \right] \quad (54)$$

$$\mathbf{p}(\mathbf{x}; t) = \int_{\mathbf{v}} f_+ \mathbf{v} + \mathcal{O} \left[\frac{m_-}{m_+} \right] \quad (55)$$

$$E(\mathbf{x}; t) = \int_{\mathbf{v}} f_+ \frac{1}{2} \|\mathbf{v}\|^2 + \mathcal{O} \left[\frac{m_-}{m_+} \right] \quad (56)$$

Combining the assumptions (28) and (48), the dominant component of the Boltzmann equations take the form

$$\nabla_{\mathbf{v}} \cdot \left[C y_{\pm} f_{\pm}(\mathbf{E} + \mathbf{v} \wedge \mathbf{B}) - K n_{\pm\pm} \mathbf{C}_{\pm\pm}^{(0)} - K n_{\pm\mp} \mathbf{C}_{\pm\mp}^{(0)} \right] = \mathcal{O}[1] \quad (57)$$

This leading-order PDE is crucially 0th-order in \mathbf{x} and t , and can, in theory, be solved pointwise in \mathbf{x} and t . For this system to be well-posed, it is necessary that the moments corresponding to mass, momentum and energy—as in Lemma 2.3—are 0. This can be guaranteed by the introduction of the following bulk forcing and heating/dissipation terms to the right-hand side (RHS) of each equation:

$$\begin{aligned} & \nabla_{\mathbf{v}} \cdot \left[C y_{\pm} f_{\pm}(\mathbf{E} + \mathbf{v} \wedge \mathbf{B}) - K n_{\pm\pm} \mathbf{C}_{\pm\pm}^{(0)} - K n_{\pm\mp} \mathbf{C}_{\pm\mp}^{(0)} \right] \\ &= \frac{2}{\beta} \cdot \frac{1}{\rho_M} \nabla_{\mathbf{v}} \cdot \left[f_{\pm}^{(0)} (M^2 \rho_C \mathbf{E} + \mathbf{j} \wedge \mathbf{B}) - \nabla_{\mathbf{v}} \left[f_{\pm}^{(0)} (\mathbf{j} - M^2 \rho_C \mathbf{u}) \cdot (\mathbf{E} + \mathbf{u} \wedge \mathbf{B}) \right] \right] \\ & \quad + \mathcal{O}[1], \quad (58) \end{aligned}$$

Since, by definition, $\bar{\mathbf{j}} \not\propto q_{\pm} \bar{\mathbf{v}}$, $\frac{2}{\beta} \not\propto |C y_{\pm}|$, such that these new RHS term are no greater than the already existing left-hand side (LHS) terms. Under the given typical tokamak

operational conditions from [Wes00] as above, β takes a value of $\beta \approx 4.249 \dots \times 10^{-3}$, such that, as predicted, $\frac{2}{\beta} \not\propto |\text{Cy}_{\pm}|$.

This leading-order PDE is crucially 0th-order in \mathbf{x} and t , and can be solved pointwise in \mathbf{x} and t . One can then write the solution to the system (58) as

$$f_{\pm}(\mathbf{x}, \mathbf{v}; t) = f_{\pm}^{(0)}[\rho_{\text{M}}|_{\mathbf{x};t}, \rho_{\text{C}}|_{\mathbf{x};t}, \mathbf{p}|_{\mathbf{x};t}, E|_{\mathbf{x};t}](\mathbf{x}, \mathbf{v}; t) + \mathcal{O}\left[\frac{1}{\text{Cy}_{+}}, \frac{1}{\text{Cy}_{+}\text{Re}_{\text{f}}}\right]. \quad (59)$$

This limit is referred to as “*thermalization*”. This motivates the creation of the fluid model.

Assumption 3: Exact Thermalization

One can further the thermalization result (59) by the assumption of *exact* thermalization:

$$f_{\pm} = f_{\pm}^{(0)} \quad (60)$$

One can then derive evolution equations for ρ_{M} , ρ_{C} , \mathbf{p} , E by taking the corresponding moments of the original Boltzmann equations (25). This derives the corresponding fluid model.

Remark. *Naturally, this assumption will (almost surely) never hold true.*

There exist other interpretations by which a fluid model can be derived that do not rely so much on the exact thermalization assumption $f_s = f_s^{(0)}$ BA: [Ref, Ref, Ref, ...] however the fluid models here will be derived from this assumption, as the derivation is more concise, and better illustrates the motivation behind the kinds of models that will be considered in Chapter ??.

Let \mathbf{u} denote the mass-averaged flow velocity,

$$\mathbf{u} := \frac{1}{\rho_{\text{M}}} \mathbf{p}. \quad (61)$$

Assuming further that:

- Local collisions $\mathbf{C}_{\pm 1 \pm 2}^{(0)}$ and the resultant asymptotic distributions $f_{\pm}^{(0)}$ are isotropic, such that the 2nd and 3rd moments can be written in the forms:

$$\int_{\mathbf{v}} f_s^{(0)} \mathbf{v}^{\otimes 2} \sim \rho_{\text{M}} \mathbf{u}^{\otimes 2} + p \mathbf{I} \quad (62)$$

$$\int_{\mathbf{v}} f_s^{(0)} \mathbf{v}^{\otimes 3} \sim \rho_{\text{M}} \mathbf{u}^{\otimes 3} + p(\mathbf{u} \otimes \mathbf{I} + \dots + \mathbf{I} \otimes \mathbf{u}) \quad (63)$$

for a pressure p . BA: (Is this a safe assumption? I’ve seen bimaxwellian background distributions being used that might imply not so much, but surely the collisions are still isotropic, no?)

- Each $f_s = o[\|\mathbf{v}\|^{-5}]$ uniformly in \mathbf{v} as $\|\mathbf{v}\| \rightarrow \infty$, such that integration by parts can be applied.

the following *fluid model* is derived:

$$\partial_t \rho_M + \nabla_{\mathbf{x}} \cdot \mathbf{p} = 0, \quad (64)$$

$$M^2 \partial_t \rho_C + \nabla_{\mathbf{x}} \cdot \mathbf{j} = 0, \quad (65)$$

$$\begin{aligned} \partial_t \mathbf{p} + (\nabla_{\mathbf{x}} \cdot [\rho_M \mathbf{u}^{\otimes 2}] + \nabla_{\mathbf{x}} p) - \frac{2}{\beta} (M^2 \rho_C \mathbf{E} + \mathbf{j} \wedge \mathbf{B}) \\ = - \int_{\mathbf{v}} \left[\frac{1}{\text{Re}_{f++}} \delta \mathbf{C}_{++} + \dots + \frac{1}{\text{Re}_{f--}} \delta \mathbf{C}_{--} \right] + \mathcal{O} \left[\frac{m_-}{m_-} \right] \end{aligned} \quad (66)$$

$$\begin{aligned} \partial_t E + \nabla_{\mathbf{x}} \cdot \left[\frac{1}{2} \rho_M \|\mathbf{u}\|^2 \mathbf{u} + \frac{5}{2} p \mathbf{u} \right] - \frac{2}{\beta} \mathbf{j} \cdot \mathbf{E} \\ = - \int_{\mathbf{v}} \left[\frac{1}{\text{Re}_{f++}} \delta \mathbf{C}_{++} + \dots + \frac{1}{\text{Re}_{f--}} \delta \mathbf{C}_{--} \right] \cdot \mathbf{v} + \mathcal{O} \left[\frac{m_-}{m_-} \right] \end{aligned} \quad (67)$$

The energy equation can be reframed in terms of the pressure, p , as

$$\begin{aligned} \frac{3}{2} \partial_t p + \left(\frac{3}{2} \nabla_{\mathbf{x}} \cdot [p \mathbf{u}] + p \nabla_{\mathbf{x}} \cdot \mathbf{u} \right) - \frac{2}{\beta} (\mathbf{j} - M^2 \rho_C \mathbf{u}) \cdot (\mathbf{E} + \mathbf{u} \wedge \mathbf{B}) \\ = - \int_{\mathbf{v}} \left[\frac{1}{\text{Re}_{f++}} \delta \mathbf{C}_{++} + \dots + \frac{1}{\text{Re}_{f--}} \delta \mathbf{C}_{--} \right] \cdot (\mathbf{v} - \mathbf{u}) + \mathcal{O} \left[\frac{m_-}{m_-} \right]. \end{aligned} \quad (68)$$

References

- [] *On the Road to ITER: Milestones*. URL: <https://www.iter.org/proj/ITERMilestones> (visited on 12/02/2023).
- [] *What Will ITER Do?* URL: <https://www.iter.org/sci/goals> (visited on 12/02/2023).
- [Abe+13] I. G. Abel et al. “Multiscale Gyrokinetics for Rotating Tokamak Plasmas: Fluctuations, Transport and Energy Flows”. In: *Reports on Progress in Physics* 76.11 (Oct. 2013). DOI: 10.1088/0034-4885/76/11/116201.
- [Alf43] H. Alfvén. “On the Existence of Electromagnetic-Hydrodynamic Waves”. In: *Arkiv för Matematik, Astronomi och Fysik* 29B(2) (1943), pp. 1–7.
- [Asc06] M. Aschwanden. *Physics of the Solar Corona: An Introduction with Problems and Solutions*. en. Springer Science & Business Media, Aug. 2006. ISBN: 978-3-540-30766-2.
- [CL13] P. K. Chu and X. Lu. *Low Temperature Plasma Technology: Methods and Applications*. en. CRC Press, July 2013. ISBN: 978-1-4665-0990-0.
- [How+06] G. G. Howes et al. “Astrophysical Gyrokinetics: Basic Equations and Linear Theory”. In: *The Astrophysical Journal* 651.1 (Nov. 2006), p. 590. DOI: 10.1086/506172.

- [McK+01] G. R. McKee et al. “Non-Dimensional Scaling of Turbulence Characteristics and Turbulent Diffusivity”. In: *Nuclear Fusion* 41.9 (Sept. 2001), p. 1235. DOI: 10.1088/0029-5515/41/9/312.
- [Mea09] D. Meade. “50 Years of Fusion Research”. In: *Nuclear Fusion* 50.1 (2009). ISSN: 0029-5515. DOI: 10.1088/0029-5515/50/1/014004.
- [PBP11] F. I. Parra, M. Barnes, and A. G. Peeters. “Up-Down Symmetry of the Turbulent Transport of Toroidal Angular Momentum in Tokamaks”. In: *Physics of Plasmas* 18 (June 2011). DOI: 10.1063/1.3586332.
- [Phi95] K. J. H. Phillips. *Guide to the Sun*. en. Cambridge University Press, Mar. 1995. ISBN: 978-0-521-39788-9.
- [Pie17] A. Piel. *Plasma Physics: An Introduction to Laboratory, Space, and Fusion Plasmas*. en. Springer, Sept. 2017. ISBN: 978-3-319-63427-2.
- [Wes00] J. Wesson. *The Science of JET*. en. Mar. 2000.